Title

Deceptive Complexity in Formation of Cleistantha-8,12-diene

Journal

Organic Letters, 24(14)

ISSN

1523-7060

Authors

Liang, Jin
Merrill, Amy T
Laconsay, Croix J
et al.

Publication Date

2022-04-15

DOI

10.1021/acs.orglett.2c00680

Peer reviewed

HHS Public Access

Author manuscript

Org Lett. Author manuscript; available in PMC 2023 April 15.

Published in final edited form as:

Org Lett. 2022 April 15; 24(14): 2646–2649. doi:10.1021/acs.orglett.2c00680.

Deceptive complexity in formation of cleistantha-8,12-diene

Jin Liang[†,⊥], **Amy T. Merrill**[§,‡], **Croix J. Laconsay**[§,‡], **Anwei Hou**[¶], **Qingyu Pu**[†], **Jeroen S. Dickschat**[¶], **Dean J. Tantillo**[§], **Qiang Wang**[†,*], **Reuben J. Peters**[⊥,*]

[†]State Key Laboratory of Crop Gene Exploration and Utilization in Southwest China, College of Agronomy, Sichuan Agricultural University, Chengdu, Sichuan 611130, China

[⊥]Roy J. Carver Department of Biochemistry, Biophysics & Molecular Biology, Iowa State University, Ames, IA 50011, USA

[§]Department of Chemistry, University of California, Davis, Davis, CA 95616, USA

[¶]Kekulé-Institut für Organische Chemie und Biochemie, Rheinische Friedrich-Wilhelms Universität Bonn, 53121 Bonn, Germany

Abstract

A barley diterpene synthase (HvKSL4) was found to produce (14*S*)-cleistantha-8,12-diene (**1**). Formation of the nearly planar cyclohexa-1,4-diene configuration leaves the ring poised for aromatization, but necessitates a deceptively complicated series of rearrangements steered through a complex energetic landscape, as elucidated here through quantum chemical calculations and labeling studies.

Graphical Abstract

[*]**Corresponding Authors**: Q.W.: qwang@sicau.edu.cn; R.J.P.: rjpeters@iastate.edu.

[‡]Author Contributions

(A.T.M., C.J.L.) These authors contributed equally.

Supporting Information

The Supporting Information is available free of charge on the ACS Publications website.

Supplemental Results, Methods, Figures and Tables (PDF)

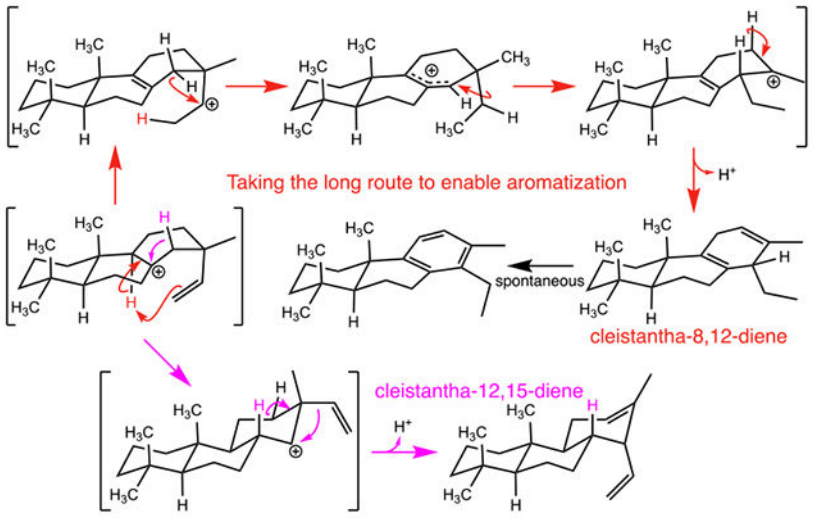

The Poaceae plant family is a particularly rich source of labdane-related diterpenoids,[1–2] which are defined by the initiation of their biosynthesis from the general diterpenoid precursor (*E,E,E*)-geranylgeranyl diphosphate (GGPP) by class II diterpene cyclases, most directly to produce the eponymous labdadienyl/copalyl diphosphate (CPP).[3] However, relatively little is known about such biosynthesis in barley (*Hordeum vulgare*), with only the *ent*-CPP synthase HvCPS1 and *ent*-kaurene synthase HvKS1 presumably involved in gibberellin phytohormone biosynthesis previously characterized.[4–5] Nevertheless, as with other cereal crop plants,[1–2] barley contains a number of genes for KS-like (KSL) terpene synthases. Among these, HvKSL4 is of particular note as its transcript accumulates in response to either UV-irradiation or infection with the fungus *Piriformospora indica*,[6] similar to KSLs involved in specialized/secondary metabolism of known importance in other Poaceae plant species.[2] Given the importance of barley as a source of drink, food and fodder, as well as the critical physiological roles for labdane-related diterpenoids in cereal resistance to biotic and abiotic stresses,[2, 7] HvKSL4 was selected for characterization of such specialized metabolism in this key crop plant.

For biochemical characterization HvKSL4 was cloned from UV-irradiated leaf tissue (see Supporting Information for details). HvKSL4 was then incorporated into a previously described modular metabolic engineering system that enables expression in Escherichia coli engineered to produce potential substrates, specifically the three known stereoisomers of CPP,[8] all of which are produced by Poaceae.[1–2] While HvKSL4 did not react with *ent*-CPP it does with both (normal) CPP (2) and *syn*-CPP. Given a recent preprint reporting that HvKSL4 is found in a biosynthetic gene cluster in the barley genome that also contains HvCPS2 that produces **2**, with derivatives of the resulting **1** found in planta,[9] this communication focuses on that reaction (see Supplemental Figure S1 for the results with *syn*-CPP). HvKSL4 reacts with **2** to form an unknown major product (Figure 1A), along with small amounts of a single minor product that was shown to be isopimara-8,15-diene (**3**) by comparison to an authentic standard (Supplemental Figure S2).

In order to identify the unknown major product (**1**) resulting from **2** additional metabolic engineering was employed to increase metabolic flux towards isoprenoids,[10] and the resulting recombinant *E. coli* grown in larger volumes. This enabled isolation of a sufficient amount of **1** (~2 mg) for structural analysis by NMR (Supplemental Table S1 and Figures S3 – S7). From this **1** is a perhydrophenanthrene tricycle with a methyl and ethyl substituent on the 'C' ring formed by HvKSL4. However, two potential configurations for the ethyl substituent and double-bond arrangement in this ring could be reasonably proposed (Supplemental Figure S8). To help determine the relevant structure, computational predictions of chemical shift data were made for both, with further consideration of the ethyl epimers, and compared to those measured (Supplemental Tables S2 – S9; all structures deposited in ioChem-BD[11]). Minimization of the mean absolute deviation (MAD) between the experimental and computed chemical shift data strongly indicated that **1** has a cleistanthane backbone with 8,12-diene arrangement, and an ethyl group in an *S* configuration (Supplemental Results S1), consistent with the C13 *iso* methyl substituent configuration observed with the minor product **3** – i.e., **1** is (14*S*)-cleistantha-8,12-diene (Figure 1B). Both UV and IR spectra are consistent with this assignment as well (Supplemental Figures S9 and S10).

Intriguingly, while terpene synthases are primarily viewed as generating specific carbon backbones via conserved reactions,[12] HvKSL4 utilizes an extended mechanism for production of a cleistanthane. In particular, this skeletal structure can be most simply formed following initiating ionization of **2** and cyclization to a pimara-15-en-8-yl carbocationic intermediate by 1,2-hydride transfer from C14 to C8, with subsequent 1,2-shift of the vinyl group from C13 to C14 prior to terminating deprotonation (e.g., green arrows in Figure 1B). However, this mechanism leaves the vinyl substituent intact, in contrast to the reduced ethyl group observed here. Accordingly, the reaction to form **1** must involve a more complex series of rearrangements.

The initial step is a relatively straightforward cyclization of **2** to form an isopimar-15-en-8-yl$^+$ intermediate (**A**), immediate deprotonation of which yields the minor product **3** (Figure 1B). Beyond the initial formation of **A**, two distinct pathways to **1** were considered here (Supplemental Results S2). These can be distinguished by initial formation of the 8-ene or 12-ene (Scheme 1). The first (pathway 1) proceeds from **A** via a 1,4-proton transfer (C14 to C16). By contrast, the second (pathway 2) proceeds via a 1,6-proton transfer (C9 to C16). While the inherent energetic barrier for the initial proton transfer has been predicted to be significantly higher for pathway 1,[13–14] it is still enzymatically surmountable, as seen with other diterpene synthases.[15–16] Nevertheless, in both pathways initial proton transfer is followed by additional rearrangement. To investigate the energetic barriers for these subsequent steps, and place these within the already computed complex energetic landscape for the resulting isopimaren-15-yl$^+$ intermediates,[13–14] further computational analyses (density functional theory calculations, mPW1PW91/6–31+G(d,p)//B3LYP/6–31+G(d,p)[17–18]) were carried out, with the results summarized in Supplemental Scheme S1. All barriers are predicted to be ≤ 30 kcal mol^{-1} for both pathways, consistent with the ~31 kcal mol^{-1} barrier to the 1,4-proton transfer with **A** catalyzed by diterpene synthases involved in conifer resin acid biosynthesis (presumably via barrier lowering),[13]

leaving open the possibility that either pathway could be utilized by HvKSL4, although pathway 2 is inherently preferred by a substantial amount.

To discern between the two pathways isotopic labeling studies were employed. Given the exogenous protonation invoked for cyclopropyl ring opening in pathway 1 (see intermediate **I** in Scheme 1), initial studies were carried out with a coupled reaction in $^{2}H_{2}O$, including initial cyclization of GGPP to **2** by a class II diterpene cyclase, which involves incorporation of a deuterium as previously shown.[19] However, the further cyclization of **2** to **1** by HvKSL4 did not lead to incorporation of an additional deuterium beyond that found in **2**, arguing against pathway 1 (Supplemental Figure S11). Nevertheless, given the frequency of intramolecular proton transfer in terpene synthase catalyzed reactions,[12] the absence of incorporation from an exogenous source does not provide definitive evidence – i.e., as the cyclopropyl might be opened by 1,4-proton transfer from C12 to C15. Accordingly, additional labeling studies were carried out. These relied on generation of labeled GGPP from farnesyl diphosphate and isopentenyl diphosphate, using a GGPP synthase, as previously described,[20–22] along with the synthesis of (15,15,15-$^{2}H_{3}$)farnesyl diphosphate reported here (Supplemental Results S3). This enabled a series of experiments to more fully investigate the predicted rearrangements (Scheme 2). First, a coupled reaction with (1-^{13}C,6-^{2}H)GGPP was carried out, which results in (16-^{13}C,9-^{2}H)-**A**, with observation of a triplet for C16 in the ^{13}C NMR spectra demonstrating derivation to (16-^{13}C,16-^{2}H)-**1** (Supplemental Figure S12). This confirms 1,6-proton transfer within **A** to form isopimara-8-en-15-yl^{+} (**B**). Notably, approximately half of the minor product **3** retains the deuterium, suggesting a mixed origin from deprotonation of either **A** at C9 (loss of ^{2}H) or **B** at C16 (retaining ^{2}H). Second, a coupled reaction with (2-^{13}C,19,19,19-$^{2}H_{3}$)GGPP was carried out, which results in (15-^{13}C,14,14-$^{2}H_{2}$)-**A**, with observation of a triplet for C15 in the ^{13}C NMR spectra demonstrating derivation to (15-^{13}C,14,15-$^{2}H_{2}$)-**1** (Supplemental Figure S13). This confirms the 1,3-proton transfer within **B** to form the allylic carbocation intermediate isopimara-8-en-14-yl^{+} (**C**). The subsequent 1,2-ethyl migration from C13 to C14 formally proceeds from **C** as isopimara-8-en-14-yl^{+} to yield the rearranged carbocation intermediate cleistantha-8-en-13-yl^{+} (**D**). Finally, a coupled reaction with (4,4-$^{2}H_{2}$)GGPP was carried out, which results in (12,12-$^{2}H_{2}$)-**A**, with observation of the loss of a deuterium in the derived (12-^{2}H)-**1** (Supplemental Figure S14). This confirms concluding deprotonation of **D** at C12 rather than intramolecular transfer.

Use of pathway 2 by HvKSL4 for production of **1** emphasizes the complexity of the energetic landscape for this reaction, which includes previously reported alternative rearrangements of **B**.[14] There are alternative transition states leading towards ring expansion (barrierless at the mPW1PW91 level of theory utilized here) or the 1,2-methyl migration leading to production of the cyclohexa-1,4-diene abietane miltiradiene (5.2 kcal mol^{-1} relative to **B**), and the inherent barriers for these are similar to that for the production of **1** (0.2 kcal mol^{-1}). Even within the relevant pathway carbocation **C** can undergo an alternative 1,2-methyl shift (leading to a cassane backbone, such as in **E** and **4**) rather than 1,2-ethyl shift (c.f. blue vs red arrows in Scheme 1), and the energetic barrier for each is essentially identical (19.9 versus 19.5 kcal mol^{-1}, respectively, relative to **C**). While the energetic barrier for the 1,2-hydride shift from C14 to C8 within the initially formed **A**

to generate the pimar-15-en-14-yl^{+} precursor to vinyl containing cleistantha-12,15-diene (Supplemental Figure S15) is greater than that for transition to **B** (14.5 versus 11.3 kcal mol^{-1}, respectively), it is still easily surmountable. Thus, HvKSL4 must steer its reaction through a complex energetic landscape in order to selectively produce **1**. This is hypothesized to enable formation of the nearly planar cyclohexa-1,4-diene ring, indicating eventual aromatization in any derived phytoalexins. Indeed, the recent preprint reports that barley produces aromatic derivatives of **1**.[9] Accordingly, the work reported here elucidates the ability of terpene synthases to not only form various carbon backbones, but specific olefin isomers that enable further transformations via use of an alternative more extended mechanism, providing an additional contribution to terpenoid natural products biosynthesis.

Supplementary Material

Refer to Web version on PubMed Central for supplementary material.

ACKNOWLEDGMENT

Financial support for the work described here was provided by the National Natural Science Foundation of China (31971825 to Q.W.), China Scholarship Council (fellowship to J.L.), NIH (GM131885 to R.J.P.), NSF (CHE-030089 via the XSEDE program to D.J.T.) and DFG (DI1536/7-2 to J.S.D.). We also thank Andreas Schneider (Univ. Bonn) for HPLC-UV analysis of **1**.

REFERENCES

1. Zi J; Mafu S; Peters RJ, To gibberellins and beyond! Surveying the evolution of (di)terpenoid metabolism. Annu Rev Plant Biol 2014, 65, 259–86. [PubMed: 24471837]
2. Murphy KM; Zerbe P, Specialized diterpenoid metabolism in monocot crops: Biosynthesis and chemical diversity. Phytochemistry 2020, 172, 112289. [PubMed: 32036187]
3. Peters RJ, Two rings in them all: the labdane-related diterpenoids. Nat Prod Rep 2010, 27 (11), 1521–30. [PubMed: 20890488]
4. Wu Y; Zhou K; Toyomasu T; Sugawara C; Oku M; Abe S; Usui M; Mitsuhashi W; Chono M; Chandler PM; Peters RJ, Functional characterization of wheat copalyl diphosphate synthases elucidates the early evolution of labdane-related diterpenoid metabolism in the cereals. Phytochemistry 2012, 84, 40–46. [PubMed: 23009878]
5. Zhou K; Xu M; Tiernan MS; Xie Q; Toyomasu T; Sugawara C; Oku M; Usui M; Mitsuhashi W; Chono M; Chandler PM; Peters RJ, Functional characterization of wheat ent-kaurene(-like) synthases indicates continuing evolution of labdane-related diterpenoid metabolism in the cereals. Phytochemistry 2012, 84, 47–55. [PubMed: 23009879]
6. Li L; Chen X; Ma C; Wu H; Qi S, Piriformospora indica requires kaurene synthase activity for successful plant colonization. Plant Physiol Biochem 2016, 102, 151–60. [PubMed: 26943021]
7. Zhang J; Li R; Xu M; Hoffmann RI; Zhang Y; Liu B; Zhang M; Yang B; Li Z; Peters RJ, A (conditional) role for labdane-related diterpenoid natural products in rice stomatal closure. New Phytol 2021.
8. Cyr A; Wilderman PR; Determan M; Peters RJ, A modular approach for facile biosynthesis of labdane-related diterpenes. J Am Chem Soc 2007, 129 (21), 6684–5. [PubMed: 17480080]
9. Liu Y; Balcke GU; Porzel A; Mahdi L; Scherr-Henning A; Bathe U; Zuccaro A; Tissier A, A barley gene cluster for the biosynthesis of diterpenoid phytoalexins. bioRxiv 2021, DOI: 10.1101/2021.05.21.445084.
10. Morrone D; Lowry L; Determan MK; Hershey DM; Xu M; Peters RJ, Increasing diterpene yield with a modular metabolic engineering system in E. coli: comparison of MEV and MEP isoprenoid precursor pathway engineering. Appl. Microbiol. Biotechnol 2010, 85, 1893–1906. [PubMed: 19777230]

11. Alvarez-Moreno M; de Graaf C; Lopez N; Maseras F; Poblet JM; Bo C, Managing the computational chemistry big data problem: the ioChem-BD platform. J Chem Inf Model 2015, 55 (1), 95–103. [PubMed: 25469626]
12. Christianson DW, Structural and Chemical Biology of Terpenoid Cyclases. Chem Rev 2017, 117 (17), 11570–11648. [PubMed: 28841019]
13. Hong YJ; Tantillo DJ, A potential energy surface bifurcation in terpene biosynthesis. Nature chemistry 2009, 1 (5), 384–9.
14. Hong YJ; Tantillo DJ, Biosynthetic consequences of multiple sequential post-transition-state bifurcations. Nature chemistry 2014, 6 (2), 104–11.
15. Ravn MM; Coates RM; Flory JE; Peters RJ; Croteau R, Stereochemistry of the cyclization-rearrangement of (+)-copalyl diphosphate to (−)-abietadiene catalyzed by recombinant abietadiene synthase from Abies grandis. Org Lett 2000, 2 (5), 573–6. [PubMed: 10814381]
16. Ravn MM; Coates RM; Jetter R; Croteau R, Stereospecific intramolecular proton transfer in the cyclization of geranylgeranyl diphosphate to (−)-abietadiene catalyzed recombinant cyclase from grand fir (Abies grandis). Chem Commun (Camb) 1998, 1998, 21–22.
17. Lee C; Yang W; Parr RG, Development of the Colle-Salvetti Correlation-Energy Formula into a Functional of the Electron Density. Phys Rev B 1988, 37, 785–789.
18. Adamo C; Barone V, Exchange Functionals with Improved Long-range Behavior and Adiabatic Connection Methods without Adjustable Parameters: The mPW and mPW1PW Models. J. Chem. Phys 1998, 108, 664–675.
19. Potter KC; Jia M; Hong YJ; Tantillo D; Peters RJ, Product Rearrangement from Altering a Single Residue in the Rice syn-Copalyl Diphosphate Synthase. Org Lett 2016, 18 (5), 1060–3. [PubMed: 26878189]
20. Rabe P; Rinkel J; Dolja E; Schmitz T; Nubbemeyer B; Luu TH; Dickschat JS, Mechanistic Investigations of Two Bacterial Diterpene Cyclases: Spiroviolene Synthase and Tsukubadiene Synthase. Angew Chem Int Ed Engl 2017, 56 (10), 2776–2779. [PubMed: 28146322]
21. Rinkel J; Lauterbach L; Dickschat JS, A Branched Diterpene Cascade: The Mechanism of Spinodiene Synthase from Saccharopolyspora spinosa. Angew Chem Int Ed Engl 2019, 58 (2), 452–455. [PubMed: 30426646]
22. Mitsuhashi T; Rinkel J; Okada M; Abe I; Dickschat JS, Mechanistic Characterization of Two Chimeric Sesterterpene Synthases from Penicillium. Chemistry 2017, 23 (42), 10053–10057. [PubMed: 28671289]

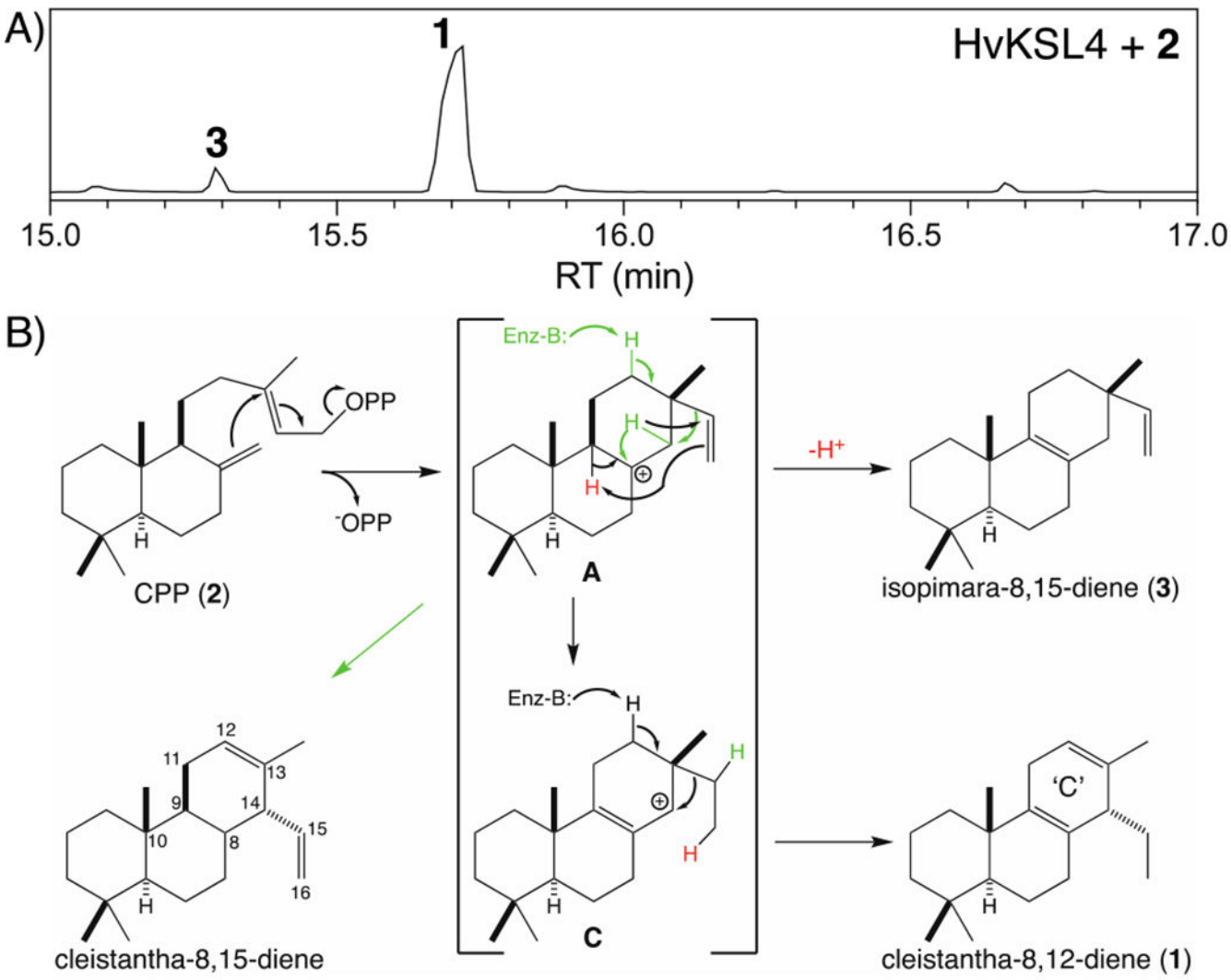

Figure 1.

HvKSL4 activity with CPP (**2**). A) Total ion chromatogram for extract from *E. coli* expressing HvKSL4 and also engineered to produce CPP (**2**), with peak numbering as described in the text. B) Scheme showing **2** and reaction leading to identified products, as well as 'simpler' alternative also leading to a cleistanthadiene (green arrows), as discussed in the text.

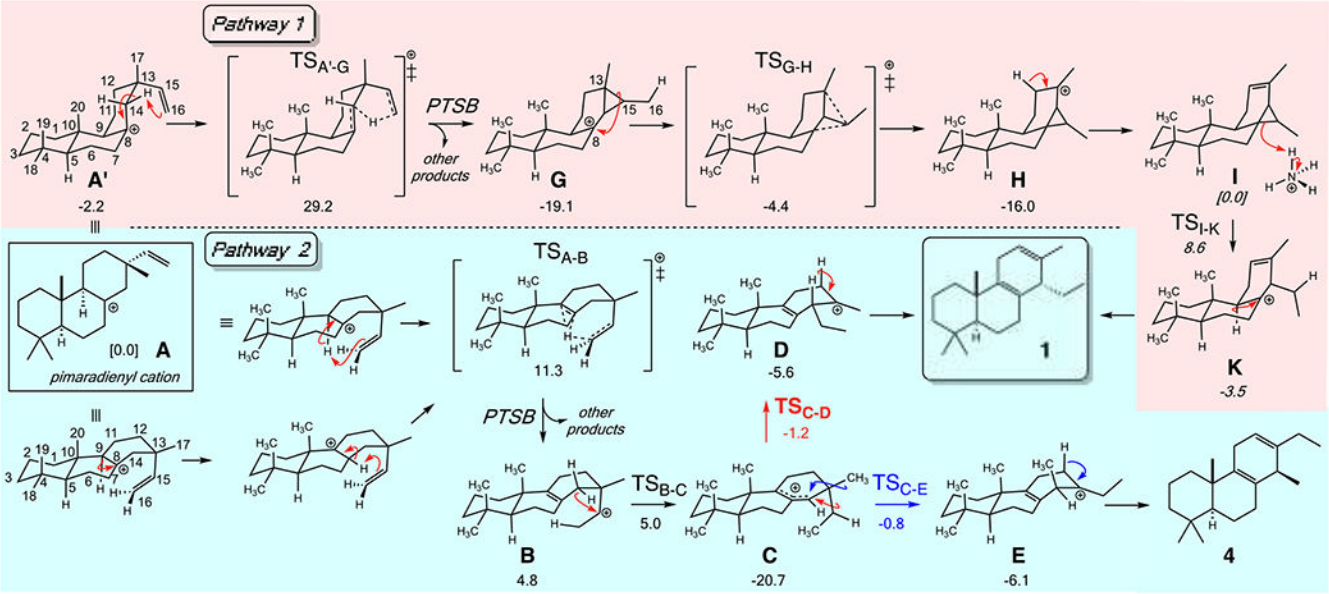

Scheme 1. Alternative pathways for the production of 1[f]

[f]Pathway 1 (top, shaded in red) and pathway 2 (bottom, shaded in blue). Also indicated are relative energies (kcal mol^{-1}) of minima and transition state structures calculated using density functional theory (mPW1PW91/6-31+G(d,p)//B3LYP/6-31+G(d,p)). In both pathways the initial proton transfer exhibits a post-transition state bifurcation (PTSB) leading to other products (and sometimes other PTSBs), as previously described.[13–14]

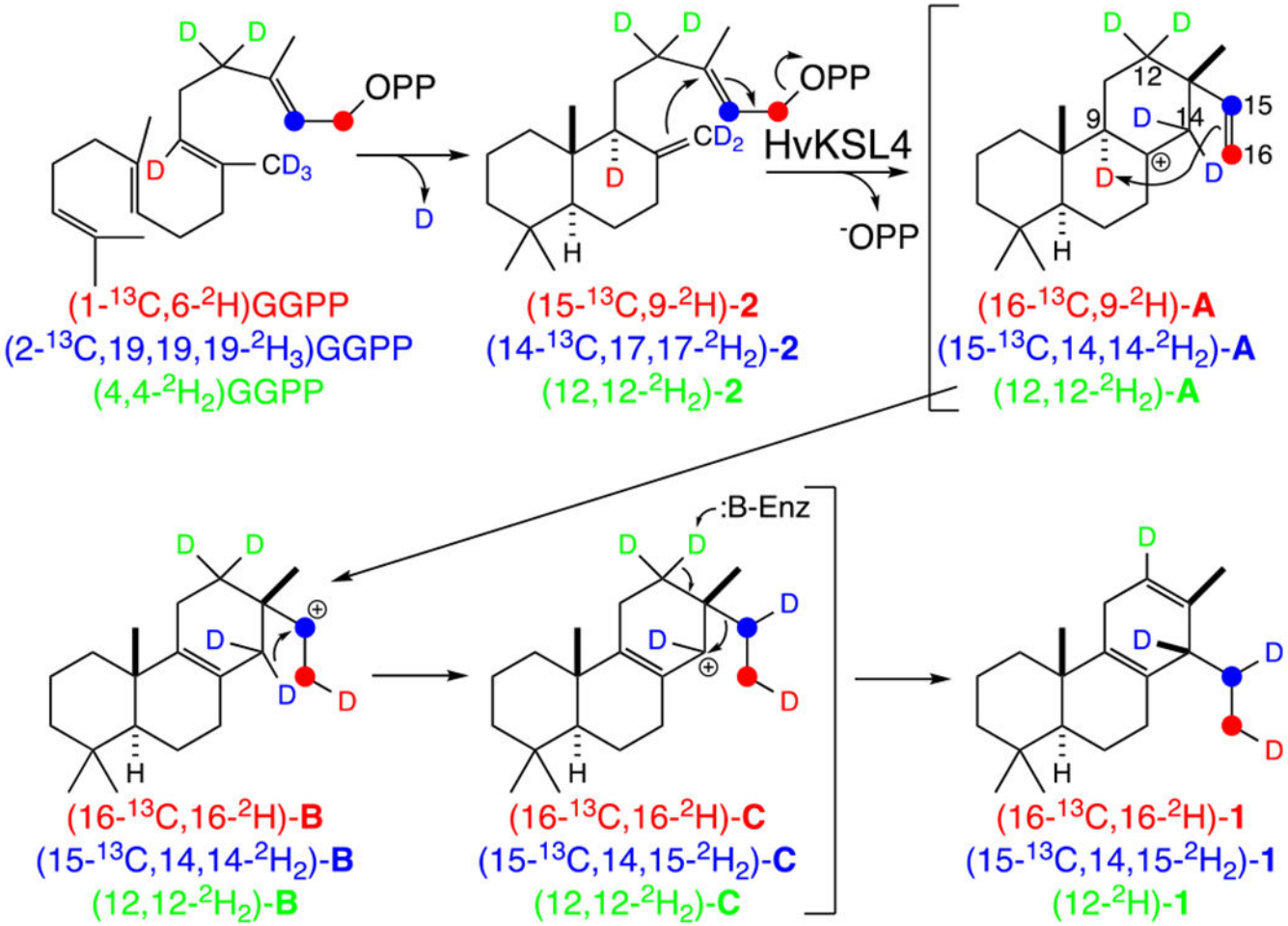

Scheme 2. Labeling studies of HvKSL4 production of 1[f]

[f]Shown for the relevant pathway 2.